Effect of Single and Multiple Injections of Adipose Stem Cells and Ascorbic Acid on the Cerebral Cortex: Histological Study in Experimentally Induced Type I Diabetes

Original Article

Maha Baligh Zickri[1], Dalia Hussein Helmy[2], Asmaa Mahmoud Mostafa[2] and Azza Saleh Embaby[2]

Department of Medical Histology and Cell Biology, Faculty of Medicine, [1]Cairo University, [2]Beni-Suef University, Egypt

ABSTRACT

Introduction: Alzheimer's Disease (AD) is common cause of dementia in the world. The link connecting AD and Diabetes mellitus (DM) appears so strong that AD is referred as Brain Diabetes. Adipose-derived mesenchymal stem cells (AMSCs) played a potential role in stem cell transplantation in animal models. The aim of this study was to evaluate and compare the possible therapeutic effect of both single and multiple injections of AMSCs and ascorbic acid (AA) on the cerebral cortex in induced type1 DM (T1DM) in adult male albino rats.

Materials and Methods: Forty four adult male albino rats were divided into, Group I (Control group) of 5 rats. Group II (Diabetic group). Group III (Diabetic treated with AMSCs single injection) .Group IV (Diabetic treated with AMSCs single injection and AA) each 7 rats and received single intra peritoneal (IP) injection of STZ 50 mg/kg, in Group III and Group IV, 1x106 AMSCs, were injected IV, in Group IV oral AA of 500mg/Kg was added. Group V (Diabetic treated with AMSCs multiple injection) and Group VI (Diabetic treated with AMSCs multiple injection and AA) each 7 rats, each was injected IV by 1ml of AMSCs four times, in Group VI combined daily oral administration of AA was performed. Histological, immunohistochemical, morphometric and statistical studies were performed.

Results: Group II demonstrated multiple large masses exhibiting dark nuclei in the External pyramidal (EP) layer, deformed neurons, rarified neuropil. Group III recruited minimal amelioration of the previous changes. Group IV showed better changes. Group V recruited obvious improvement. Group VI revealed minimal changes.

Conclusion: T1DM induced cerebral cortical inflammatory and degenerative changes. AMSCs proved a therapeutic effect that was more noticeable in response to multiple injections. Combined AA and AMSCs therapy guaranteed the most remarkable effect that can be related to activated migration and trans-differentiation.

INTRODUCTION

Diabetes Mellitus (DM) is a severe metabolic disorder in which hyperglycemia is caused by insulin secretion or insulin action defects, or both[1].

The most popular causes of dementia in the world today are Alzheimer's disease (AD) and other progressive neurodegenerative diseases. Millions of patients are thought to be affected around the world[2]. A recent study found that there was a higher chance of dementia, but not Parkinson's disease or amyotrophic lateral sclerosis[3].

The relation between AD and DM appears to be so strong that it has been proposed that AD be classified as a neuroendocrine condition known as "Diabetes Type 3" or "Brain Diabetes"[4]. Insulin deficiency has been confirmed as a possible link in the chain[5].

Reactive oxygen species (ROS) build up in diabetics, interfering with normal cellular function. Ascorbic acid (AA) and other cellular antioxidants can help to restore the balance of antioxidant protection[6].

The application of stem cell therapies to diabetes care has opened up new possibilities. Mesenchymal stem cells (MSCs) have been shown to be an interesting therapeutic choice among all types of stem cells, centred on their immunomodulatory properties and differentiation potentials, which have been shown in a variety of laboratory and clinical trials. From different sources, MSCs have been studied for their ability to transform into insulin-producing cells[7].

Adipose-derived mesenchymal stem cells (AMSCs) showed promise as seeding cells in stem cell transplantation in animal models[8]. Antioxidants are thought to cause the stemness of cells[9].

The aim of this study was to assess and compare the potential therapeutic effects of single and multiple injections of AMSCs and ascorbic acid on the cerebral cortex in adult male albino rats with induced type 1 diabetes

MATERIALS AND METHODS

Drugs

- Sigma Company (St. Louis, MO, USA) provided streptozotocin (STZ) in a powder form as a 1 g vial. A digital scale was used to weigh the appropriate dosage, which was then dissolved in citrate buffer.

- Development of Chemical Industries (Giza, Egypt) provided ascorbic acid (AA) in the form of 1g Vitacid C effervescent tablets. The requisite doses were weighed and dissolved in water using a digital scale.

Experimental Design

The rats used in this study were 44 adult male albino rats weighing 200 grams on average. They were held in clean, well-ventilated rooms in sanitary stainless steel cages at Cairo University's Faculty of Medicine's Animal House of Physiology Department. They were given unlimited food and water. Both procedures were carried out in accordance with Cairo University's guidelines. The rats were split into six groups:

AMSCs were isolated from four rats in the donor group.

(Control group) Group I: It consisted of 5 rats that corresponded to the study classes II, III, IV, V, and VI and as a result, they were sacrificed.

- The first rat was given a single intraperitoneal (IP) injection of 0.5 mL citrate buffer, followed by an 8-week period of no treatment.

- A single IP injection of 0.5 ml citrate buffer was provided to the second rat. It was given 1ml of phosphate buffered saline (PBS) intravenous (IV) through the tail vein once (4 weeks later) and then left for another 4 weeks without treatment.

- For four weeks, the third rat received the same citrate buffer and PBS as the second rat, as well as daily oral AA dissolved in 0.5 ml water using a syringe without a needle.

- The fourth rat got the same citrate buffer and PBS as the second and third rats, but four times through the tail vein (on start of weeks 5, 6, 7, 8).

- For four weeks, the fifth rat was given the same citrate buffer and PBS as the fourth rat, as well as daily oral AA dissolved in 0.5 ml water using a syringe without a needle.

All control rats were sacrificed 8 weeks after the experiment start.

(Diabetic group) Group II: There were seven rats in all.

Diabetes was initiated by giving each rat a single intraperitoneal injection of STZ at a dose of 50 mg/kg body weight[10] dissolved in 0.5 ml citrate buffer. Diabetes was confirmed three days after STZ injection by testing blood glucose levels in the Biochemistry Department of Cairo University's Faculty of Medicine. If the animals' blood glucose level was greater than 200 mg/dl, they were classified as diabetic[11].

The rats were not given any treatment for 8 weeks.

(Diabetic treated with AMSCs single injection group) Group III: Diabetes was induced and confirmed in this group of 7 rats, just as it was in group II.$1x10^6$ cultured and labelled rat AMSCs[12] were injected once into the tail vein in 1ml PBS[13]. Four weeks after STZ injection (on the start of the fifth week)[14]. The Clinical Pathology Department of Cairo University's Faculty of Medicine conducted stem cell isolation, culture, marking, and phenotyping. AMSCs isolation was performed from the rat abdomen according to[15]. The culture and marking of AMSCs is carried out in accordance with[16]. The rats were not offered any further medication for another four weeks.

(Diabetic treated with AMSCs single injection and AA group) Group IV: There were seven rats in all. As in groups II and III, diabetes was induced and confirmed. 1ml of cultured and labelled AMSCs were isolated, suspended, and injected as in group III four weeks after STZ injection. Regular (daily) oral administration of 500 mg of AA per kilogram of body weight[17] dissolved in 0.5 ml of water for another 4 weeks using a syringe without a needle for each of the 7 rats.

(Diabetic treated with AMSCs multiple injection group) Group V: Diabetes was induced and confirmed in 7 rats, as in groups II, III, and IV. 1ml of cultured and labelled rat AMSCs were isolated and injected into the tail vein four weeks after STZ injection as in group III and IV, but four times (on start of weeks 5, 6, 7, 8)[18].

(Diabetic treated with AMSCs multiple injection and AA group) Group VI: There were seven rats in all. In groups II, III, IV, and V, diabetes was induced and confirmed.1ml of cultured and labelled AMSCs were isolated and injected as in group V four weeks after STZ injection. For another 4 weeks, each of the 7 rats received a concomitant daily oral administration of AA using a syringe without a needle.

8 weeks after the experiment start, animals of groups II, III, IV, V, and VI were sacrificed.

Before the sacrifice, blood samples from the tail vein were taken at the end of the eighth week to estimate blood glucose levels. At the end of the study, the animals in the control and experimental groups were sacrificed by cervical dislocation. The temporal regions of the skull were opened with a bone cutter. The brain was exposed and immediately dissected, and the frontal lobes[19] were removed after 48 hours at room temperature in 10% formol saline. Paraffin wax was used to embed frontal lobe specimens. Coronal pieces with a thickness of 5 μm[20] were processed.

In the Histology Department of Cairo University's Faculty of Medicine, sections were subjected to the following tests:

A. Measurement of fasting blood glucose level.

B. Hematoxylin and eosin (H&E) histological research[21].

C. Histochemical Investigation:

1. The amyloid plaques were examined in Congo red (CR) stain[22].

2. Prussian blue (Pb) stain to display the iron oxide-labeled ADSCs injected[23].

D. Immunohistochemical Study:

1. Synaptophysin immunostaining[24] for neuron structural function organization.

2. Endogenous and exogenous undifferentiated MSCs are detected using CD44 immunostaining[25].

E. Morphometric Analysis:

1. Glial cell mean area

2. Neurons mean area that have been deformed.

3. Masses mean area that are CR positive (+ve).

4. Count of Pb+ve cells.

5. Area% of synaptophysin +ve immunoexpression (IE).

6. Count of CD44 +ve cells.

F. Statistical Analysis[26].

RESULTS

General Observations

In the present study, two rats died at the beginning of the experiment, two days following STZ injection and they were compensated. Lethargy and polyuria were observed in groups II, III, IV, V, and VI, which improved by the end of the experiment in groups III, IV, V, and VI. The following results were recorded.

Data from in *vitro* experiments AMSCs and transfected AMSCs were mostly spindle-shaped, and immunostaining revealed a +ve membranous brownish reaction for CD44 and a -ve reaction for CD34. Flow cytometry immunophenotyping of AMSCs revealed that 96 percent of the cells were CD44 positive.

Animal Data

A) Serological Results

In comparison to the control and other experimental classes, group II was significantly more in the mean value. In comparison to control and groups IV, V, and VI, there was a substantial rise in group III.

Furthermore, as opposed to control and group VI, there was a significantly rise in groups IV and V (Table 1, Histogram 1).

B) Histological Results:Haematoxylin and Eosin (H&E) stained sections

Group I included five rats, cerebral cortex sections obtained from all control rats showed the same histological picture. The layers, nerve cells, and neuropil appeared normal in most of fields. The six layers of the cerebral cortex were molecular, external granular, external pyramidal, internal granular, internal pyramidal, and pleomorphic. Pyramidal cells with pyramidal cell bodies and thick branching dendrites at the apex were visible in the external pyramidal (EP) layer. Pyramidal cells came in a range of sizes. Stellate cells had small star-shaped cell bodies with dendrites projecting in all directions for short distances. Glial cells were detected in the neuropil that appeared as a fibrillar eosinophilic material formed of dense network of branching processes. The cytoplasm of glial cells was poorly visualized (Figure 1A).

Sections belonging to group II demonstrated multiple large acidophilic masses surrounded by clear areas in the EP layer in multiple sections. In some sections, some neurons appeared with acidophilic cytoplasm, in addition to some deformed neurons. There were also large acidophilic masses with several dark nuclei and a clear space surrounding them. Among the rare neuropil and glial cell proliferation, only a few stellate and pyramidal neurons were found (Figure 1B). Some other sections recruited obvious proliferation of glial cells exhibiting elongated nuclei among deformed neurons and rarified neuropil. Multiple fields of rarified neuropil showed multiple neurons with acidophilic cytoplasm, several deformed neurons, and glial cell proliferation.

Some fields of group III recruited small masses surrounded by clear areas in the EP layer of the cerebral cortex sections, in addition to congested vessels that were found.

By close observation, a small mass with dark nuclei that surrounded by a clear area, Multiple sections revealed some neurons with acidophilic cytoplasm, deformed neurons, and pyramidal and stellate neurons (Figure 1C).

In certain sections of the rat cerebral cortex of group IV, they revealed few very small masses surrounded by clear areas in the EP layer. A closer examination recruited few deformed neurons as well as few neurons with acidophilic cytoplasm surrounded by clear areas. Focal rarefaction of neuropil was noticed among pyramidal and stellate neurons (Figure 1D).

In certain sections of the rat cerebral cortex, group V recruited few very small masses surrounded by clear areas in the EP layer. A closer examination revealed few deformed neurons as well as a few neurons with acidophilic cytoplasm. Focal rarefaction of neuropil was noticed among pyramidal and stellate neurons (Figure 1E).

Sections in the rat cerebral cortex of group VI revealed focal areas of rarified neuropil and no obvious masses among the different layers. By closer observation, few

deformed neurons were seen. Focal rarefaction of neuropil was noticed among pyramidal, duplicated pyramidal and stellate neurons (Figure 1F).

B) 1- Congo Red Stain: Examination of sections in the cerebral cortex of rats group I ,the EP layer showed dull red staining of the neurons as well as the neuropil (Figure 2A).

Multiple strongly positive (+ve) masses of various sizes, large and tiny, were observed among the EP layer neurons in the rat cerebral cortex of group II (Figure 2B).

When sections of the rat cerebral cortex were examined, it was recruited that group III had less strongly +ve and smaller masses in the EP layer than group II (Figure 2C).

In comparison to rats in groups II and III, sections of the cerebral cortex of group IV rats revealed few strongly +ve small masses in the EP layer (Figure 2D).

Sections belonging to group V were comparable to group IV (Figure 2E).

No obvious +ve masses were detected among the dull stained neurons and neuropil by examination of various sections of group VI in the cerebral cortex of rats (Figure 2F).

Prussian Blue stain

In the EP layer of the cerebral cortex of group I rats, negative (-ve) staining with Prussian blue (Pb) was observed among pyramidal and stellate cells (Figure 3A).

In the EP layer of the cerebral cortex, sections of the rat cerebral cortex of group II displayed -ve staining among the neurons and large masses surrounded by clear regions (Figure 3B).

In the EP layer of the cerebral cortex, sections of the rat cerebral cortex of group III revealed few Pb +ve spindle cells among the neurons, as well as small masses surrounded by clear regions (Figure 3C).

In the EP layer of the cerebral cortex of group IV , there were few Pb +ve spindle cells among the neurons, as well as a few small masses surrounded by clear areas (Figure 3D).

Multiple Pb +ve spindle cells were found among the neurons in sections of the rat cerebral cortex of group V, as well as few small masses surrounded by clear areas in the EP layer of the cerebral cortex (Figure 3E).

In the EP layer of the cerebral cortex, sections of the rat cerebral cortex of group VI revealed multiple Pb +ve spindle cells among the pyramidal and stellate cells (Figure 3F).

C) Immunohistochemical Results

1. Synaptophysin immunostaining: sections of the cerebral cortex of group I rats revealed a high level of +ve immune expression (IE) among multiple pyramidal neurons in the EP layer (Figure 4A).

In the EP layer of the cerebral cortex of group II rats, sections revealed minimal +ve IE among accidental pyramidal neurons and multiple masses (Figure 4B).

Few pyramidal neurons in the EP layer of the cerebral cortex in group III rat cerebral cortex sections display mild +ve IE (Figure 4C).

Some pyramidal neurons in the EP layer of the cerebral cortex showed clear +ve IE in sections of the rat cerebral cortex from groups IV and V (Figures 4D, 4E).

Multiple pyramidal neurons in the EP layer showed extensive +ve IE when sections of the cerebral cortex of rats from group VI were examined (Figure 4F).

2- Anti-CD44 immunostained sections: the cerebral cortex of group I rats revealed negative IE with CD44 antibody among the neurons and neuropil in the EP layer (Figure 5A).

Few CD44 +ve spindle cells fused with a few neurons, as well as blood vessels and the EP layer neuropil, were found in the rat cerebral cortex of group II (Figure 5B).

Sections of the cerebral cortex of group III rats revealed some +ve spindle cells fused with few neurons, as well as blood vessels and the EP layer neuropil (Figure 5C).

In group IV, several +ve spindle cells fused with a few neurons were found in blood vessels and the neuropil of the EP layer of the cerebral cortex (Figure 5D).

Multiple +ve spindle cells fused with some neurons were found in the EP layer of the cerebral cortex of rats in group V (Figure 5E).

Sections of the cerebral cortex of group VI rats revealed numerous +ve spindle cells fused with multiple neurons, as well as in the EP layer's neuropil (Figure 5F).

D)Morphometric Results

Glial cell mean area increased significantly in group II compared to other groups, as well as in group III compared to control, groups IV, V, and VI. In addition, as compared to control and group VI, there was a large increase in groups IV and V (Table 2 , Histogram 2).

In comparison to the other experimental classes, group II had increased significantly in the mean area of deformed neurons. Furthermore, as opposed to groups IV, V, and VI, there was more rise in group III.

In comparison to group VI, there was a significant rise in groups IV and V (Table 3 , Histogram 3).

Group II had a significant increase in the mean region of CR +ve masses as compared to the other experimental classes. In comparison, as compared to groups IV and V, group III had a large increase in mean area (Table 4 , Histogram 4).

In comparison to groups IV, V, and VI, the number of Pb +ve cells was significantly lower in group III. Furthermore, a significant decrease was seen in group IV when compared to groups V and VI, while a significant decrease was found in group V when compared to group VI (Table 5, Histogram 5).

Group II had a significantly lower mean area of +ve IE than groups I, IV, V, and VI, and group III had a significantly lower mean area of +ve IE than groups I, V, and VI.

In comparison to groups I and VI, however, there was a substantial decline in group IV. Finally, by comparing groups I and VI, there was a substantial decline in group IV (Table 6, Histogram 6).

Group II had a significantly lower mean count of CD44 +ve cells than the other groups, and group III had a significantly lower mean count of CD44 +ve cells than groups V and VI. In addition, as compared to group VI, there was a substantial decline in groups IV and V (Table 7, Histogram 7).
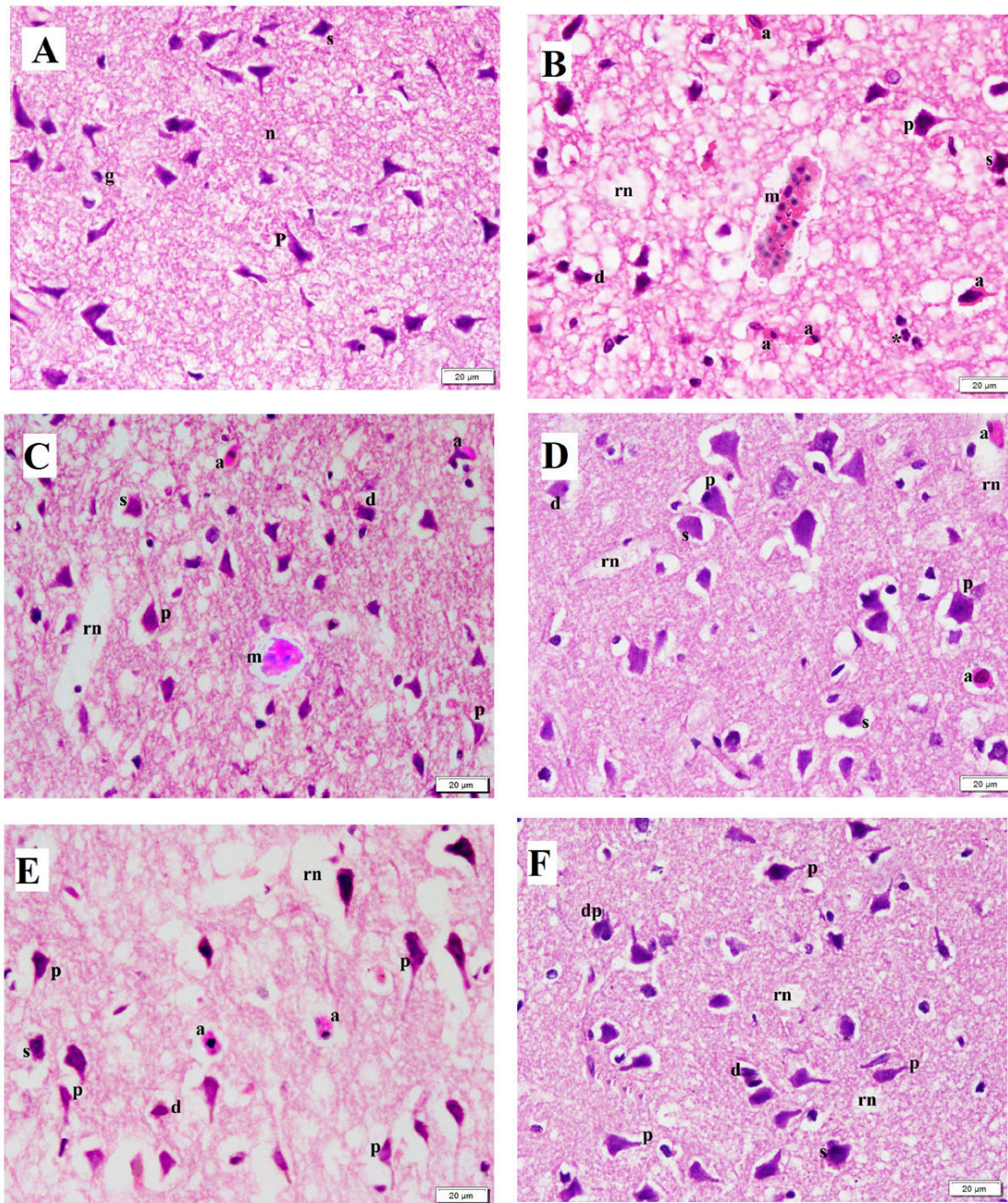

Fig. 1: A: Photomicrograph of a section of the group I rat cerebral cortex showing multiple pyramidal (P) and stellate (s) neurons, as well as glial cells (g) in the EP layer's neuropil (n). **B:** group II showing some neurons with acidophilic cytoplasm (a) , some deformed neurons (d), a large acidophilic mass (m) with numerous dark nuclei surrounded by clear space. There are only a few stellate (s) and pyramidal (P) neurons in addition to rarified neuropil (rn) and glial cells proliferation (*). **C:** group III showing a small mass (m) with dark nuclei surrounded by a clear zone, some neurons with acidophilic cytoplasm (a), deformed (d) neurons , rarified neuropil (rn), neurons of the pyramidal (P) and stellate (s) types. **D:** group IV displaying few deformed (d) neurons as well as few neurons with acidophilic cytoplasm (a) surrounded by clear areas. Note focal rarefaction of neuropil (rn),Pyramidal (P) and stellate (s) neurons are two types of neurons. **E:** group V displaying a few deformed (d) neurons as well as a few neurons with acidophilic cytoplasm (a)surrounded by clear areas. Focal rarefaction of neuropil (rn), neurons of the pyramidal (P) and stellate (s) types can be noticed. **F:** group VI showing few deformed (d) neurons , focal rarefaction of neuropil (rn), pyramidal (P), duplicated pyramidal (dp) and stellate (s) neurons (H&E, x400) .
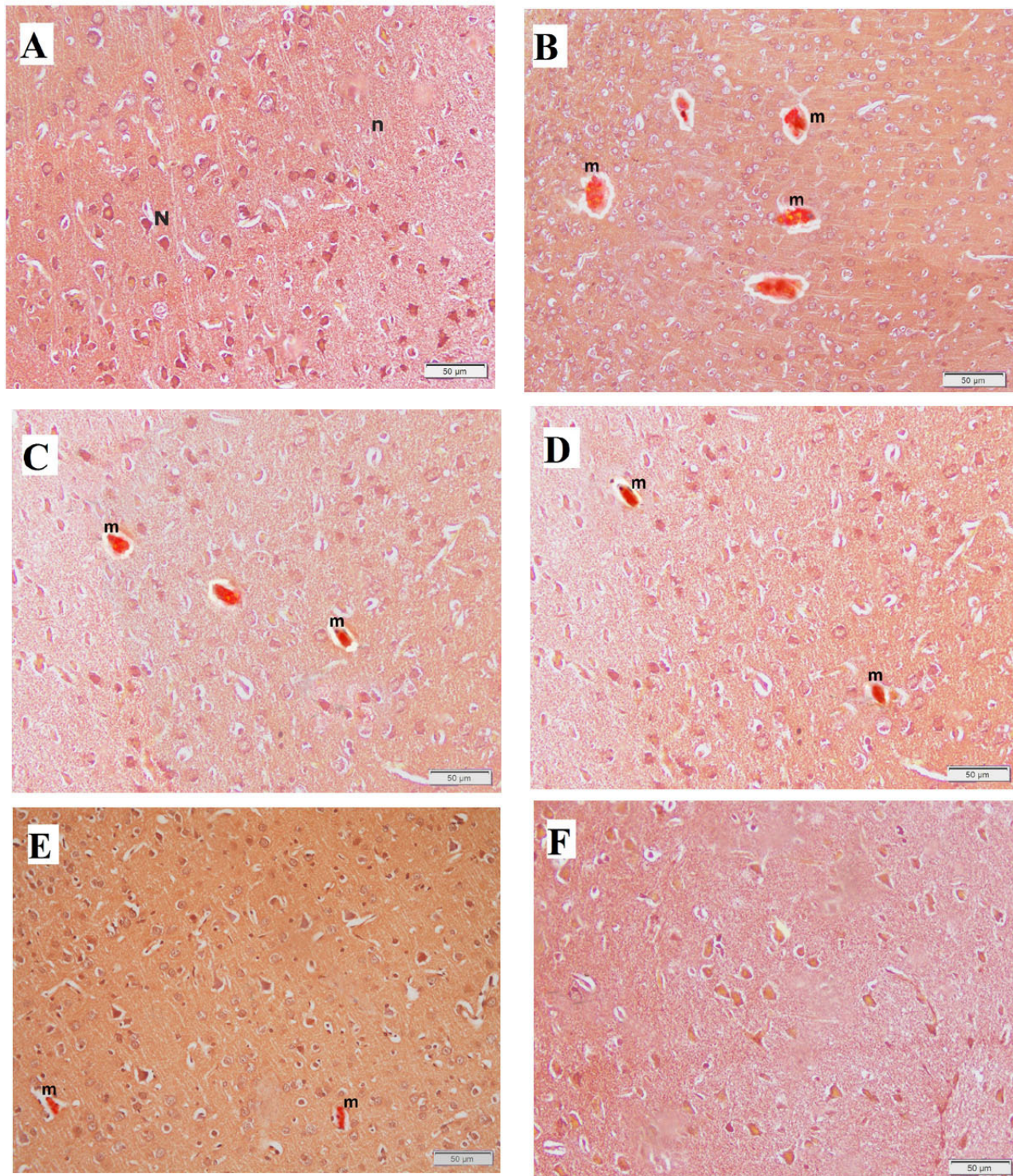
2

Fig. 2: A: Photomicrograph of a section of the group I rat cerebral cortex with dull Congo red (CR) staining of neurons (N) and neuropil (n) in the EP layer. **B:** group II showing multiple strongly +ve large and small masses (m) between the neurons and neuropil of the EP layer. **C:** group III demonstrates some strongly +ve smaller masses (m) among the neurons and neuropil of the EP layer. **D:** group IV has a few strongly positive small masses (m) in the EP layer. **E:** group V showing the EP layer with small masses (m) that are strongly positive. **F:** group VI showing no obvious strongly +ve masses among the dull stained neurons and neuropil in EP layer (CR, x200).
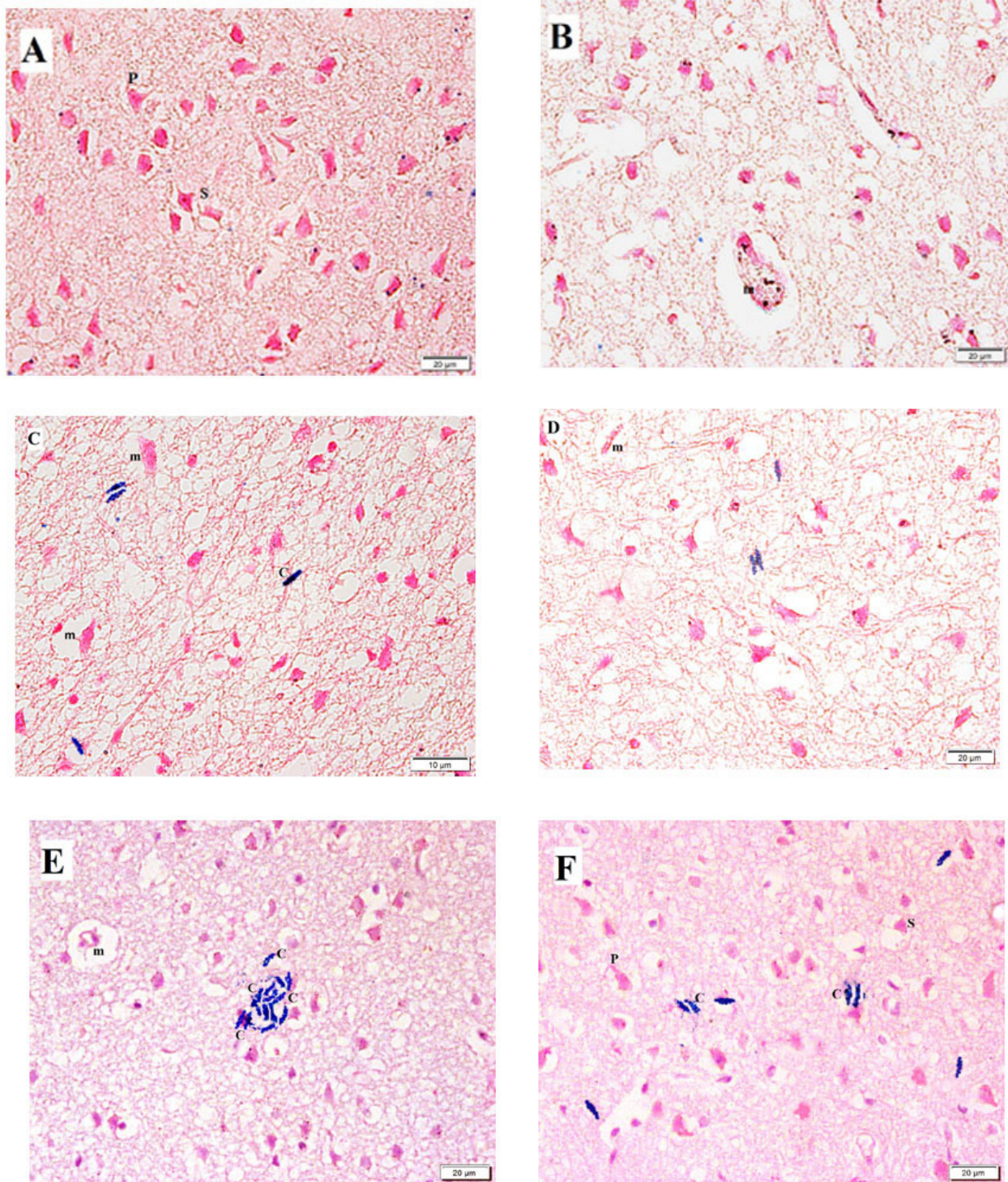
Fig. 3: A: Photomicrograph of a section of the group I rat cerebral cortex showing –ve Pb staining in pyramidal (p) and stellate (s) cells in the EP layer. **B:** group II showing -ve Pb staining among neurons in the EP layer. Note the large mass (m) surrounded by clear area. **C:** group III showing few Pb +ve cells (C) among neurons and small masses (m) surrounded by clear area in the cerebral cortex's EP layer. **D:** group IV showing that there are few Pb +ve spindle cells (C) among the neurons, as well as few small masses (m) surrounded by clear areas seen in the EP layer of the cerebral cortex. **E:** group V demonstrating the presence of multiple Pb +ve spindle cells (C) among the neurons and few small masses (m) surrounded by clear areas seen in the EP layer of the cerebral cortex. **F:** group VI showing multiple Pb +ve spindle cells   among the pyramidal and stellate seen in the cerebral cortex's EP layer (Prussian blue, x400).
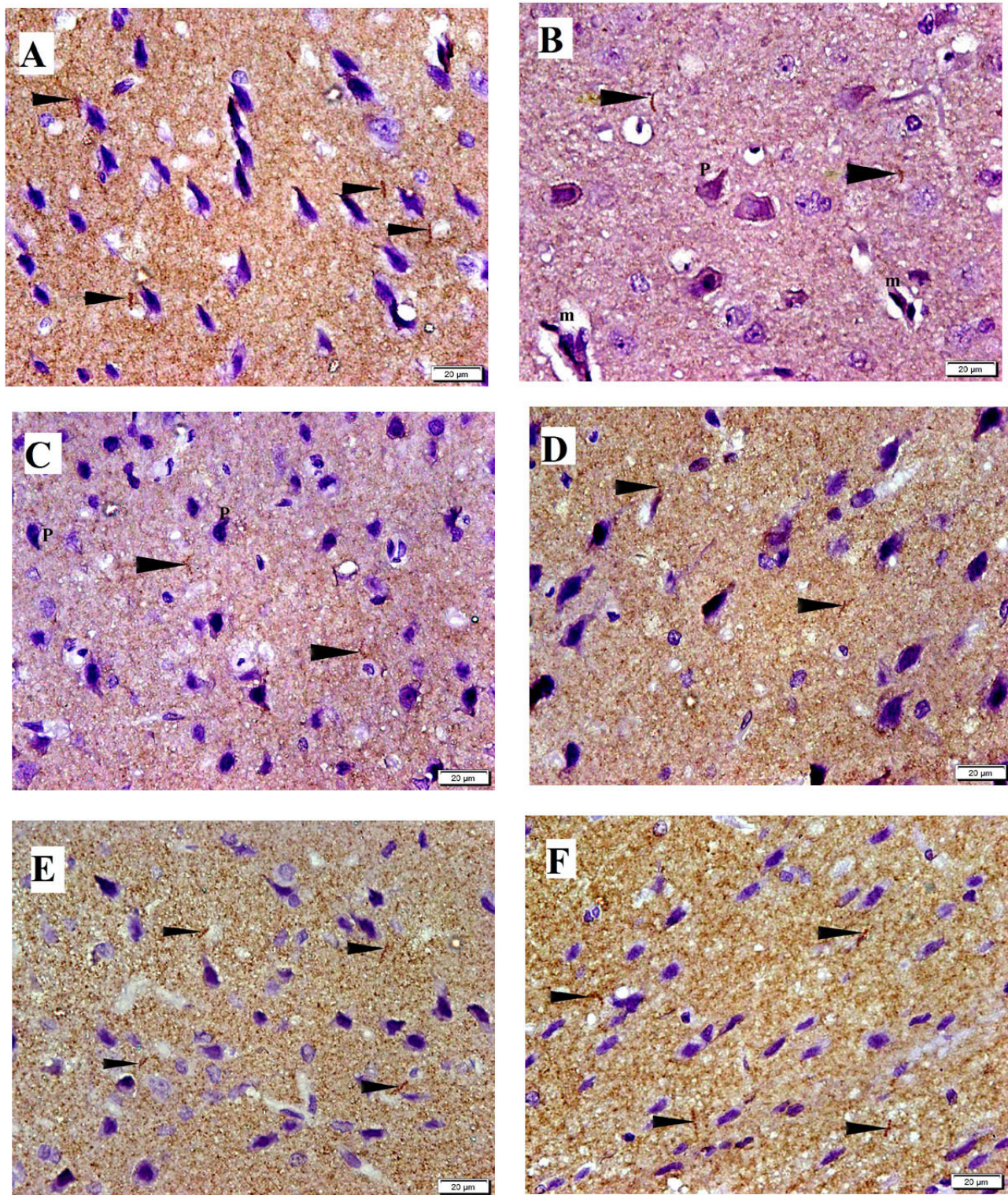
Fig. 4: A: A photomicrograph of a section of group I rat cerebral cortex showing the EPL demonstrating extensive +ve IE (arrowheads) among multiple pyramidal neurons. **B:** group II showing the EPL demonstrating minimal +ve IE (arrowheads) among pyramidal neurons (P) and multiple masses (m). **C:** group III showing the EPL demonstrating moderate +ve IE (arrowheads) among few pyramidal neurons (P). **D:** group IV showing the EPL displaying obvious positive IE (arrowheads) between some pyramidal neurons . **E:** group V showing the EPL displaying obvious positive IE (arrowheads) between some pyramidal neurons. **F:** group VI showing the EPL demonstrating extensive +ve IE (arrowheads) among multiple pyramidal neurons. (Synaptophysin immunostaining x 400)
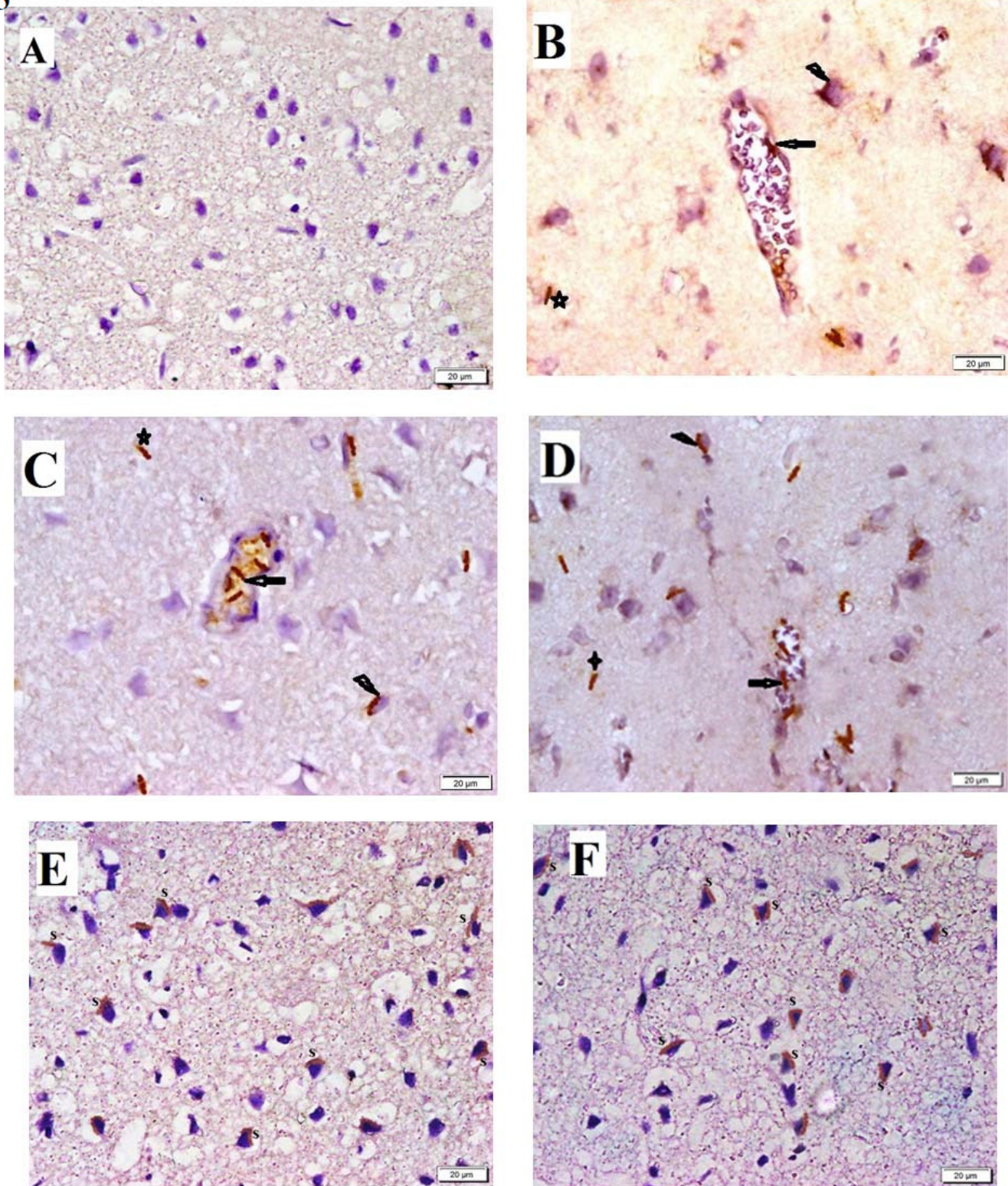
Fig. 5: A: Section of the group I rat cerebral cortex showing –ve immunostaining among different types of neurons, and the neuropil in EP layer. **B:** group II demonstrates some +ve spindle cells fused with a few neurons (arrowhead), overlying a mass (arrow), and in the neuropil (star) in EP layer. **C:** Multiple +ve spindle cells overlying a mass (arrow), fused with a few neurons (arrowhead), and in the neuropil (star) in the EP layer are shown in group III. **D:** group IV showing multiple +ve spindle cells, overlying a mass (arrow), fused with few neurons (arrowhead) and in the neuropil (star) layer of the EP layer. **E:** group V showing numerous +ve spindle cells (s) were found in the neuropil and were fused with a few neurons in the EP layer. **F:** group VI demonstrates numerous +ve spindle cells (s) in the neuropil that are fused with a few neurons in the EP layer. (Anti-CD44 Immunostaining, x400)

Table 1: Mean Fasting Blood Glucose Level in control and experimental groups

Group	FBG 3 days following STZ injection (*P value*)	FBG 8 weeks following STZ injection (*P value*)
Group I	122.8 mg/dl	114.4 mg/dl
Group II	228.5 (0.000 vs I)*	332 mg/dl(0.000 vs I,IV,V,VI)#
Group III	221.3 mg/dl (0.000 vs I)*	231 mg/dl(0.000 vs I,IV,V,VI)•^
Group IV	220.1 mg/dl (0.000 vs I)*	191.3 mg/dl (0.000 vs I, VI)•
Group V	217.7 mg/dl (0.000 vs I)*	182.3 mg/dl (0.000 vs I, VI)•
Group VI	220.6 mg/dl (1.000 vs I)*	129.5 mg/dl

* Significant compared to group I (*P* < 0.05).
\# Significant compared to the other groups (*P* < 0.05).
♦ Significant compared to groups I, VI (*P* < 0.05).
^ Significant compared to groups IV, V (*P* < 0.05).

Table 2: Mean area of glial cells in control and experimental groups

Group	Mean area (*P value*) (µ²)
Group I	2.98
Group II	18.22 (0.000 vs I, III, IV, V &VI)*
Group III	10.08 (0.000 vs I, IV, V &VI)•
Group IV	7.69 (0.935 vs V & 0.000 vs I & VI)•
Group V	7.39 (0.000 vs I & VI)#
Group VI	3.08 (1.000 vs I)

* Significant compared to groups I, III, IV, V, VI (*P* < 0.05).
♦ Significant compared to groups I, IV, V, VI (*P* < 0.05).
• Significant compared to groups I & VI (*P* < 0.05).
\# Significant compared to groups I & VI (*P* < 0.05).

Table 3: Mean area of deformed neurons in control and experimental groups

Group	Mean area (*P value*) (µ²)
Group I	-
Group II	124.57 (0.001vs III & 0.000 vs IV, V &VI)*
Group III	92.07 (0.000 vs IV, V &VI)•
Group IV	57.11 (0.992 vs V & 0.001 vs VI)•
Group V	53.75 (0.002 vs VI)#
Group VI	23.01

* Significant compared to groups I, III, IV, V, VI (*P* < 0.05).
♦ Significant compared to groups I, IV, V, VI (*P* < 0.05).
• Significant compared to groups I & VI (*P* < 0.05).
\# Significant compared to groups I & VI (*P* < 0.05).

Table 4: Mean area of CR+ve masses in control and experimental groups

Group	Mean area (*P value*) (µ²)
Group I	-
Group II	603.91 (0.000vs III, IV, V &VI)*
Group III	275.90 (0.000 vs IV, V &VI)♦
Group IV	165.12 (0.919 vs V & 0.000 vs VI)
Group V	181.76 (0.000 vs VI)
Group VI	-

* Significant compared to groups I, III, IV, VI (*P* < 0.05).
♦ Significant compared to groups I, IV, V, VI (*P* < 0.05).
• Significant compared to groups I & VI (*P* < 0.05).
\# Significant compared to groups I & VI (*P* < 0.05).

Table 5: Mean count of Prussian blue +ve cells in control and experimental groups

Group	Mean count (*P value*)
Group I	-
Group II	-
Group III	3.5 (0.000 vs IV, V &VI)•
Group IV	5.3 (0.032 vs V & 0.000 vs VI)•
Group V	6.3 (0.000 vs VI)#
Group VI	10.1

♦ Significant compared to groups I, IV, V, VI (*P* < 0.05).
• Significant compared to groups I & VI (*P* < 0.05).
\# Significant compared to groups I & VI (*P* < 0.05).

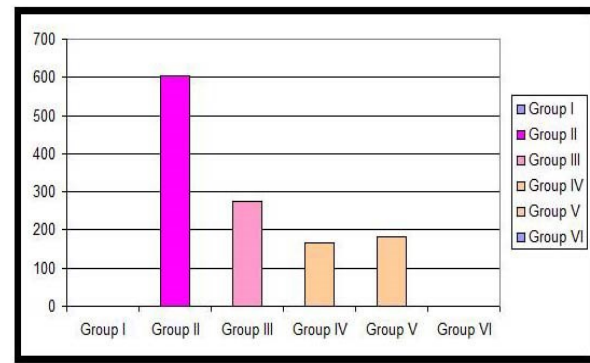**Table 6:** Mean area % of synaptophysin +ve IE in control and experimental groups

Group	Mean area %
Group I	1.30
Group II	0.14 (0.731 vs III & 0.002 vs IV 0.000 vs I, V &VI)*
Group III	0.28 (0.095 vs IV & 0.021 vs V & 0.000 vs I & VI)•
Group IV	0.54 (0.991 vs V & 0.000 vs I & VI)•
Group V	0.60 (0.000 vs I & VI)#
Group VI	1.16

* Significant compared to groups I, III, IV, V, VI (*P* < 0.05).
♦ Significant compared to groups I, IV, V, VI (*P* < 0.05).
• Significant compared to groups I & VI (*P* < 0.05).
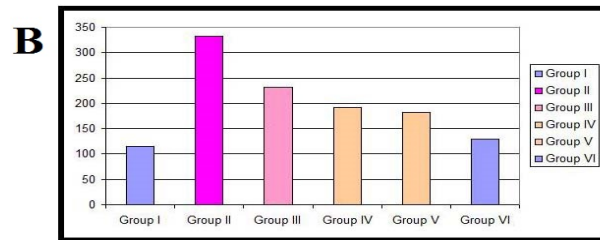\# Significant compared to groups I & VI (*P* < 0.05).

Table 7: Mean count of CD44 +ve cells in control and experimental groups

Group	Mean count (*P value*)
Group I	-
Group II	1.7 (0,000 vs III,IV,V & VI)*
Group III	4.8 (0.280 vs IV, 0.002 vs V & 0.000 vs VI)♦
Group IV	5.5 (0.280 vs V & 0.000 vs VI)•
Group V	6.2 (0.000 vs VI)#
Group VI	7.8

* Significant compared to groups I, III, IV, V, VI ($P < 0.05$).
♦ Significant compared to groups I, IV, V, VI ($P < 0.05$).
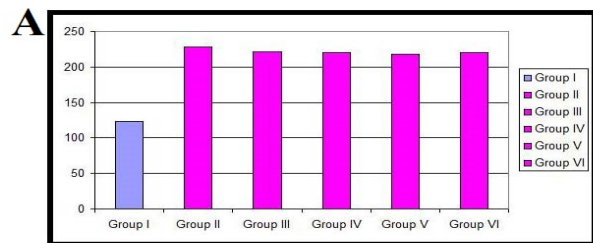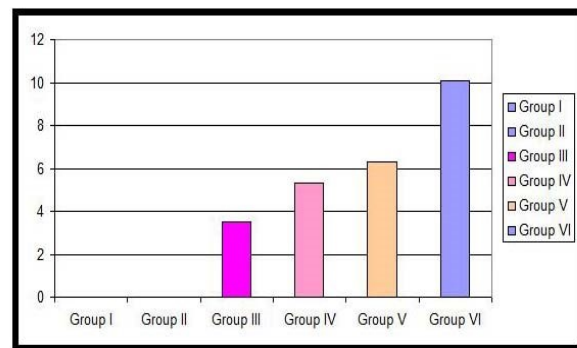• Significant compared to groups I & VI ($P < 0.05$).
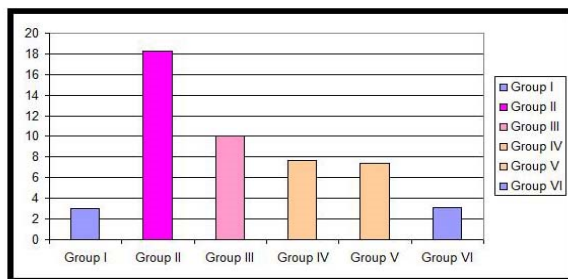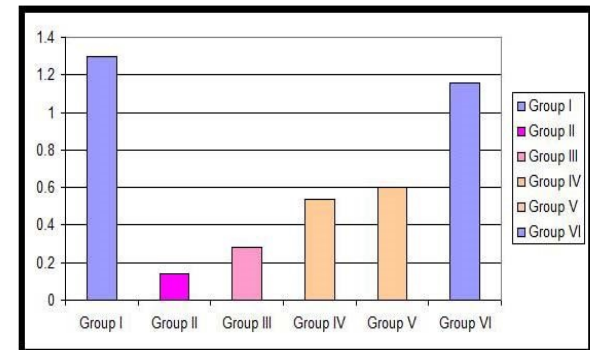# Significant compared to groups I & VI ($P < 0.05$).

Histogram 1: A: Mean FBG Level 3 days following STZ injection in groups (control and experimental). **B:** Mean FBG Level 8 weeks following STZ injection in control and experimental groups.

Histogram 2: Mean area of glial cells in control and experimental groups.

Histogram 3: Mean area of deformed neurons in control and experimental groups.

Histogram 4: Mean area of CR +ve masses in control and experimental groups.

Histogram 5: Mean count of Prussian blue +ve cells in control and experimental groups.

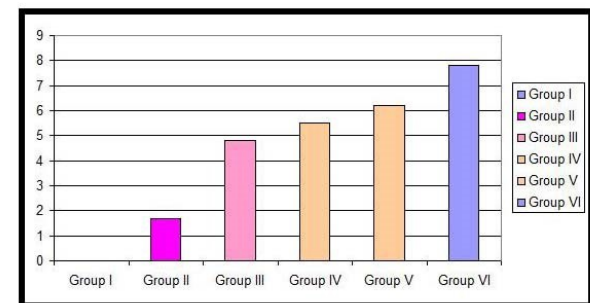**Histogram 6:** Mean area % of Synaptophysin +ve IE in control and experimental groups.

Histogram 7: Mean count of CD44 +ve cells in control and experimental groups.

DISCUSSION

The effects of AA and AMSCs on the morphological changes in the cerebral cortex complicating STZ-induced DM in rats were demonstrated in this research. Serological, histological, histochemical, immunohistochemical, morphometric and statistical findings all supported this.

In this study, the diabetic group (group II) had significantly higher mean blood glucose levels than the control and other experimental groups.

Furthermore, at an optimal dose (50 to 75 mg/kg, intraperitoneal), STZ is one of the most commonly used chemical agents for inducing type 1 diabetes in rats[27].

In this study, sections of the cerebral cortex of diabetic rats from group II (diabetic group) were examined and revealed multiple large acidophilic masses surrounded by clear areas and exhibiting multiple dark nuclei in the EP layer of the cerebral cortex,

Multiple acidophilic cytoplasm neurons and some deformed neurons, as shown by a significant increase in the mean area of deformed neurons. These findings suggested neuron degeneration and fusion of degenerated neurons, which may signal the start of a mass or plaque formation. The frontal cortex is involved in vision, according to other studies, and In Alzheimer's disease, it's believed to be impacted in humans[28].

These results matched those of Garman (2011), who characterised the classic appearance of neuron degeneration as "acute eosinophilic neuron degeneration"[29]. Neuronal shrinkage is seen in neurodegenerative diseases, and eosinophilic neurons indicate ischemic/hypoxic damage, according to Kovacs (2015)[30]. Other researchers also discovered that as neurodegeneration progresses, the number of pyramidal cells decreases[31].

According to Luebke *et al*., (2010), layer III (EP) pyramidal neurons are the primary neurons involved in and mediating many cognitive functions of the frontal cortex. In neurodegenerative disorders, they can be targeted selectively[32]. Increased development and/ or exposure to reactive oxygen species(ROS) for an extended period of time can disrupt cellular homeostasis, leading to cell death, according to Bradley-Whitman *et al*. (2014)[33].

According to other studies, the amyloid (A) peptide produced by abnormal proteolytic cleavage of the amyloid precursor protein (APP) is toxic to neurons and synapses , explaining the mechanism of neuronal death in AD, which is the most common ND[34]. Hyperphosphorylation and aggregation of the microtubule-associated protein tau are also facilitated by A , according to others[35].

Previous research had found a high number of amyloid masses in the frontal cortex's upper layers. Human brain scans showing ND, on the other hand, revealed masses in the parietal and temporal cortices[36]. Extracellular neuritic amyloid masses are a primary neuropathological hallmark of ND, according to Biron *et al*. (2013)[34]. The amyloid

masses in the cortex were detected using H&E of ND patients[30].

Group II showed apparent proliferation of glial cells with elongated nuclei. In the current research, a significant increase in the mean area of glial cells confirmed this hypothesis.

According to a previous study, microglia are attracted to masses in ND and showed high levels of proinflammatory cytokines and reactive oxygen species (ROS)[37]. Others have shown that tumor-necrosis factor- (TNF-) activated microglia are toxic to terminally differentiated neurons[38].

EP layer revealed neuropil vacuolation in group II in the current study. This is in line with a study that found that as a result of neuronal process swelling, the neuropil adjacent to degenerating neurons may become finely vacuolated[29].

There is strong evidence that DM plays a role in the development of ND[39]. This is in line with Wang *et al* (2014) 's results, that showed increased amyloid reactivity in the frontal cortex of STZ-induced diabetic rats.

Furthermore, excess glucose is metabolised by alternate metabolic pathways, which may cause direct neurotoxicity[40]. Since STZ does not cross the BBB, Nazem *et al*. (2015) concluded that the deficits observed by Wang *et al*. (2014) were caused by the peripheral effects of the drug[41].

In the present study, the masses were confirmed to be of an amyloid nature by CR staining which demonstrated multiple strongly +ve large and small masses among the neurons of EP layer of group II. These findings were backed up by a significant increase in the mean area of amyloid plaques in group II compared to the other experimental groups. They also demonstrated that the CR stain is used to determine if amyloid plaques are beta sheet or not which agrees with previous findings[42].

In the current work, minimal +ve synaptophysin IE were found in EP layer in group II, the mean area percent was decreased significantly as compared to the groups . The preceding findings supported the structural and functional changes in neurons, as well as the loss of synaptic proteins. Others have shown that synapse density, a key indicator of synaptic efficiency, is represented by synaptophysin immunoreactivity.in agreement with previous findings[43]. Diabetes has been linked to cognitive dysfunction as a result of changes in excitatory neurotransmitter expression[44].

According to Rachmany *et al*, (2017), in brain injured animals, synaptophysin immunoreactivity was found to be significantly lower in the temporal brain region[45].

In this work, group II recruited a small number of CD44 +ve spindle cells fused with a few neurons in the EP layer's neuropil and within blood vessels. According to Ma *et al*., (2014), tissue damage is often linked to the activation of inflammatory cells, which is consistent with previous findings. Inflammatory molecules orchestrate microenvironmental changes that lead to MSC mobilization

and differentiation. These MSCs may be tissue-resident endogenous MSCs or BM-derived MSCs[46]. Diabetes, according to other researchers, has a detrimental effect on the functional properties of tissue-resident SCs[47].

In the present work, group III (Diabetic Group treated with single injection of AMSCs) revealed congested vessels, small masses of dark nuclei surrounded by bright areas in the EP layer, less neurons with acidophilic cytoplasm, less deformed neurons and rarified neuropil compared to group II. AMSCs therapy appeared to reverse mediated diabetic degenerative changes, according to previous findings. This result was consistent with Gerace *et al*. (2017), who revealed that allowing MSCs to move to areas of injury improved T1DM outcomes and altering the microenvironment to facilitate cell survival and regeneration[48].

Group III recruited fewer strongly CR +ve and smaller masses in EP layer, few Pb +ve spindle cells, +ve synaptophysin IE among few pyramidal neurons, and in blood vessels and the EP layer's neuropil, some CD44 +ve cells fused with a few neurons. MSCs, according to Lin *et al*. (2017), not only as a source of progenitors for cell replacement however, stimulate local cells through paracrine stimulation to aid tissue regeneration[49]. The use of multipotent MSCs, even in a single injection, has been recognised as a potential treatment option for a variety of degenerative disease according to Ding *et al*, (2017)[50].

Groups IV (Diabetic group treated with single injection of AMSCs and AA) and V (Diabetic group treated with multiple injections of AMSCs) showed few very small masses surrounded by clear areas in the EP layer, few neurons with deformed cytoplasm, few neurons with acidophilic cytoplasm surrounded by clear areas, and focal rarefaction of neuropil.

The previous findings were supported by a substantial decrease in the mean area of deformed neurons and glial cells as compared to group III. The previous findings proved a more noticeable therapeutic effect of AA combined with a single AMSCs injection and of that of multiple AMSCs injections compared to group III. Other research has shown that administration of AA contributes to tissue regeneration and homeostasis in normal tissues and organs, so clinical studies have shown that AA can help delay the development of neurodegenerative diseases[51].

Groups IV and V compared to group III, there was a significant decrease in the mean area of CR strongly +ve amyloid plaques. Sil *et al*. (2016) studied the function of AA in neurodegeneration and memory deficit in Alzheimer's disease and found similar results. The authors found that administering AA (400 mg/kg) to AD rats improved memory impairments. However, AD rats given 600 mg/kg of AA had worse memory impairment As a result, it appears that AA has an antioxidant effect at low doses and causes prooxidant/neurotoxic effects at higher doses[52].

Sections in groups IV and V in EP layer showed a significant reduction in the mean area percent of synaptophysin +ve IE when compared to group III. Moretti *et al*. (2017) reported that the effects of AA in ND work primarily by lowering oxidative stress and preventing protein aggregate formation, additionally, improving synaptic transmission[51].

Groups IV and V demonstrated multiple Pb +ve and CD44 +ve spindle cells in the neuropil, fused with neurons in the EP layer. In comparison to groups II and III, there was a significant increase in the mean area percent of CD44 +ve cells in groups IV and V. When compared to group III. This can be explained by the possibility of AA activation of endogenous MSCs. It was reported that AA causes SC migration and differentiation in a previous study[53]. They demonstrated the potent synergistic effects of the combination on SC differentiation by developing a multiple injection transplantation strategy using tail vein injections and transplantation reduced diabetic complications[54].

Group VI (Diabetic Group treated with multiple injections of AMSCs and AA) revealed focal areas of rarified neuropil and few deformed neurons

A significant reduction in the mean area of deformed neurons and the mean area of glial cells was revealed when compared to groups III, IV, and V.

This remarkable improvement in neurodegenerative changes could be attributed to the beneficial effects of SC-based therapy reported by Mahmoud *et al*, (2019). They documented potential improvement of multiple intra-articular injections of allogeneic BMMSCs were used to treat knee lesions caused by surgically induced osteoarthritis in an animal study. BMMSCs secrete growth factors that mediate the trophic actions in multiple allogeneic intra-articular injections[55].

Group VI revealed no obvious CR +ve masses. They noted that recent SCs could be used to treat or modulate ND, according to preclinical evidence, which they agreed with. SC-mediated anti-amyloidogenesis and replacement of lost neurons are among the mechanisms of SC-based therapies for ND, according to the previous study[56].

In the present study, group VI, multiple Pb +ve cells were found among the neurons in EP layer.The number of Pb +ve cells was significantly higher in comparison to the other experimental groups. They found that injecting hADSCs via the BBB and allowing them to move into the brain improved cognitive function in the ND mouse model, confirming previous findings[57]. Devitt *et al*. (2015) confirmed ADSCs' ability to differentiate into neural cells, expanding their usefulness to the treatment of brain injury through their powerful paracrine signalling mechanisms in neurodegeneration[58].

Sections in group VI demonstrated numerous CD44 +ve cells in EP layer, fused with multiple neurons and in the neuropil. Group VI had a significant increase in the mean area percent of CD44 +ve cells when compared to groups III, IV, and V. This is explained by the activation of endogenous SCs by the therapeutic cells in addition to more

differentiation of SCs in group VI with multiple injections and by the effect of combined AA administration. Others also verified this, stating that ADSCs and MSCs share the CD44 marker[59]. Liu *et al*. (2013) reported that MSCs distributed systemically can cross the BBB in the event of injury or inflammation which explains MSC homing to the brain.The cerebral vasculature's integrity, on the other hand, is likely to be impaired following injury, which may lead to passive MSC accumulation[60]. Multiple intravenous injections of MSCs enter the brain and treat mice with inflammation-induced brain damage and memory loss, in accordance with Lykhmus *et al*. (2019)[61].

CONCLUSION

It can be concluded that T1DM induced cerebral cortical inflammatory and degenerative morphological changes. AMSCs proved a definite therapeutic effect that was more noticeable in response to multiple injections. Combined AA and AMSCs therapy guaranteed the most remarkable effect that can be related to activated migration and trans-differentiation.

RECOMMENDATIONS

1. A longer duration using AA treatment is recommended before sacrifice for more accurate evaluation of the therapeutic effect of AA.

2. Possible comparative studies between other anti inflammatory therapies and AA therapy for treatment of different types of neurodegeneration.

3. The need for study of the therapeutic effect of AA in clinical studies on volunteer subjects serving the medical field.

4. A possible comparative study between the effect of endogenous and therapeutic stem cells may be of value.

5. Study the therapeutic effect of MSCs from different sources on other types of neurodegeneration.

CONFLICT OF INTERESTS

There are no conflicts of interest.

REFERENCES

1. Fujimaki S, Wakabayashi T, Takemasa T, Asashima M, and Kuwabara T (2015): Diabetes and Stem Cell Function. Biomed Res Int, 2015: 592915-592930.

2. Nowrangi MA, Lyketsos CG and Rosenberg PB (2015): Principles and management of neuropsychiatric symptoms in Alzheimer's dementia. Alzheimers Res Ther, 7: 12-21.

3. Raj R, Kaprio J, Korja M, Mikkonen ED, Jousilahti P and Siironen J (2017): Risk of hospitalization with neurodegenerative disease after moderate-to-severe traumatic brain injury in the working-age population: A retrospective cohort study using the Finnish national health registries. PLoS Med, 14(7): e1002316-1002331.

4. Rizvi SMD, Shaikh S, Waseem SMA, Shakil S, Abuzenadah A.M., Biswas D, Tabrez S, Ashraf GM and Kamal MA (2015): Role of anti-diabetic drugs as therapeutic agents in Alzheimer's disease. EXCLI J, 14: 684-696.

5. Velazquez R, Tran A, Ishimwe E, Denner L, Dave N, Oddo S and Dineley KT (2017): Central insulin dysregulation and energy dyshomeostasis in two mouse models of Alzheimer's disease. Neurobiol Aging, 58:1-13.

6. Seminario A, Song L, Zulet A, Nguyen HT, González EM and Larrainzar E (2017): Drought Stress Causes a Reduction in the Biosynthesis of Ascorbic Acid in Soybean Plants. Front Plant Sci, 8: 1042-1051.

7. Hashemian SJ, Kouhnavard M and Esfahani EN (2015): Mesenchymal Stem Cells: Rising Concerns over Their Application in Treatment of Type One Diabetes Mellitus. Journal of Diabetes Research: 675103-675121.

8. Zhang W, Schmull S, Du M, Liu J, Lu Z, Zhu H, Xue S, Lian F (2016): Estrogen Receptor α and β in Mouse: Adipose-Derived Stem Cell Proliferation, Migration, and Brown Adipogenesis In *Vitro*. Cell Physiol Biochem, 38(6): 2285-2299.

9. Chen J Lan J, Liu D, Backman LJ, Zhang W, Zhou Q and Danielson P (2017): Ascorbic Acid Promotes the Stemness of Corneal Epithelial Stem/Progenitor Cells and Accelerates Epithelial Wound Healing in the Cornea. Stem Cells Transl Med, 6(5): 1356-1365.

10. Hidaka R, Machida M, Fujimaki S, Terashima K, Asashima M and Kuwabara T (2013): Monitoring neurodegeneration in diabetes using adult neural stem cells derived from the olfactory bulb. Stem Cell Res Ther, 4(3): 51-61.

11. Bhansali S, Kumar V, Saikia UN, Medhi B, Jha V, Bhansali A and Dutta P (2015): Effect of mesenchymal stem cells transplantation on glycaemic profile and their localization in streptozotocin induced diabetic Wistar rats. Indian J Med Res, 142(1): 63-71.

12. Sheashaa H, Lotfy A, Elhusseini F, Abdel Aziz A, Baiomy A, Awad S, Alsayed AH, El-Gilany A, Saad MA, Mahmoud K, Zahran F, Salem DA, Sarhan A, Ghaffar HA and Sobh M (2016): Protective effect of adipose-derived mesenchymal stem cells against acute kidney injury induced by ischemia-reperfusion in Sprague-Dawley rats. Exp Ther Med, 11(5): 1573-1580.

13. Bassiony HS, Zickri MB, Metwally HG, ElSherif HA and Alghandour SM (2016): Comparative Histological Study on the Therapeutic Effect of Green Tea and Stem Cells in Rat Model of Alzheimer's Disease Complicating Diabetes. MD Thesis: 56-74.

14. Aboul-Fotouh GI, Zickri MB, Metwally HG, Ibrahim IR and Kamar SSI (2016): Comparative Study on the Therapeutic Effect of Atorvastatin and Stem Cells on Amiodarone Induced Lung Injury in Male Rat. MD Thesis: 53-76.

15. Takehara Y, Yabuuchi A, Ezoe K, Kuroda T, Yamadera R, Sano C, Murata N, Aida T, Nakama K, Aono F, Aoyama N, Kato K and Kato O (2013): The restorative effects of adipose-derived mesenchymal stem cells on damaged ovarian function. Lab Invest, 93(2): 181-193.

16. Espina M, Jülke H, Brehm W, Ribitsch I, Winter K and Delling U (2016): Evaluation of transport conditions for autologous bone marrow-derived mesenchymal stromal cells for therapeutic application in horses. PeerJ, 4: e1773-1795.

17. Picklo MJ and Thyfault JP (2015): Vitamin E and vitamin C do not reduce insulin sensitivity but inhibit mitochondrial protein expression in exercising obese rats. Appl Physiol Nutr Metab, 40(4): 343-369.

18. Kuo YR, Chen CC, Chen YC and Chien CM (2017): Recipient Adipose-derived Stem Cells Enhance Recipient Cell Engraftment and Prolong Allotransplant Survival in a Miniature Swine Hind-limb Model. Cell Transplant, 26(8):1418-1427.

19. 19. Wang JQ, Yin J, Song YF, Zhang L, Ren YX, Wang DG, Gao LP and Jing YH (2014): Brain aging and AD-like pathology in streptozotocin-induced diabetic rats. J Diabetes Res, 2014: 796840-796851.

20. Rolyan H, Scheffold A, Heinrich A, Begus-Nahrmann Y., Langkopf BH, Hölter SM, Vogt-Weisenhorn DM, Liss B, Wurst W, Lie DC, Thal DR, Biber K and Rudolph KL (2011): Brain, 134(Pt 7): 2044-2056.

21. Kiernan J K (2001): Histological and Histochemical methods . In: Theory and practice. 3rd ed., Arnold Publisher, London , New York, and New Delhy: 111-162.

22. Wilcock D, Gordon M and Morgan D (2006): Quantification of cerebral amyloid angiopathy and parenchymal amyloid plaques with Congo red histochemical stain. Nat Protoc, 1(3): 1591-1595.

23. Ellis R (2007): Perls Prussian blue Stain Protocol, Pathology Division, Queen Elizabeth Hospital: South Australia. Arch.Pathol, 39: 42.

24. Sørdal O, Qvigstad G, Nordrum IS, Sandvik AK, Gustafsson BI, Waldum H (2014): The PAS positive material in gastric cancer cells of signet ring type is not mucin. Exp Mol Pathol 28, 96(3): 274-278.

25. Cai Y, Liu T, Fang F, Xiong C and Shen S (2015): Comparisons of Mouse Mesenchymal Stem Cells in Primary Adherent Culture of Compact Bone Fragments and Whole Bone Marrow. Stem Cells International, 2015: 708906-708913.

26. Emsley R, Dunn G and White I (2010): Mediation and moderation of treatment effects in randomized controlled trials of complex interventions. Stat Methods Med Res, 19(3): 237-270.

27. Eleazu CO, Eleazu KC, Chukwuma S and Essien UN (2013): Review of the mechanism of cell death resulting from streptozotocin challenge in experimental animals, its practical use and potential risk to humans. J Diabetes Metab Disord, 12(1): 60-66.

28. Girard SD, Baranger K, Gauthier C, Jacquet M, Bernard A, Escoffier G, Marchetti E, Khrestchatisky M, Rivera S and Roman FS (2013): Evidence for early cognitive impairment related to frontal cortex in the 5XFAD mouse model of Alzheimer's disease. J Alzheimers Dis, 33(3): 781-796.

29. Garman RH (2011): Histology of the central nervous system. Toxicol Pathol, 39(1): 22-35.

30. Kovacs GG (2015): Practical approach to diagnosis: sampling and basic stains. In: Neuropathology of Neurodegenerative Diseases: A Practical Guide. Cambridge University Press, United Kingdom: 55-69.

31. Bussière T, Giannakopoulos P, Bouras C, Perl DP, Morrison JH and Hof PR (2003): Progressive degeneration of nonphosphorylated neurofilament protein-enriched pyramidal neurons predicts cognitive impairment in Alzheimer's disease: Stereologic analysis of prefrontal cortex area 9. J. Comp. Neurol, 463(3): 281-302.

32. Luebke JI, Weaver CM, Rocher AB, Rodriguez A, Crimins JL, Dickstein DL, Wearne SL and Hof PR (2010): Dendritic vulnerability in neurodegenerative disease: insights from analyses of cortical pyramidal neurons in transgenic mouse models. Brain Struct Funct, 214(2-3): 181-199.

33. Bradley-Whitman MA, Timmons MD, Beckett TL, Murphy MP, Lynn BC and Lovell MA (2014): Nucleic acid oxidation: an early feature of Alzheimer's disease. J Neurochem, 128(2): 294-304.

34. Biron KE, Dickstein DL, Gopaul R, Fenninger F and Jefferies WA (2013): Cessation of neoangiogenesis in Alzheimer's disease follows amyloid-beta immunization. Sci Rep, 3: 1354-1360.

35. Chabrier MA, Cheng D, Castello NA, Green KN and LaFerla FM (2014): Synergistic effects of amyloid-beta and wild-type human tau on dendritic spine loss in a floxed double transgenic model of Alzheimer's disease. Neurobiol Dis, 64: 107-117.

36. Valente T, Gella A, Fernàndez-Busquets X, Unzeta M and Durany N (2010): Immunohistochemical analysis of human brain suggests pathological synergism of Alzheimer's disease and diabetes mellitus. Neurobiol Dis, 37(1): 67-76.

37. Krabbe G, Halle A, Matyash V, Rinnenthal JL, Eom GD, Bernhardt U, Miller KR, Prokop S, Kettenmann H and Heppner FL (2013): Functional impairment of microglia coincides with Beta-amyloid deposition in mice with Alzheimer-like pathology. PLoS One, 8(4): e60921-60928.

38. Bhaskar K, Maphis N, Xu G, Varvel NH, Kokiko-Cochran ON, Weick JP, Staugaitis SM, Cardona A, Ransohoff RM, Herrup K and Lamb BT (2014): Microglial derived tumor necrosis factor-α drives Alzheimer's disease-related neuronal cell cycle events. Neurobiol Dis, 62: 273-285.

39. Cai Z, Yan Y and Wang Y (2013): Minocycline alleviates beta-amyloid protein and tau pathology via restraining neuroinflammation induced by diabetic metabolic disorder. Clin Interv Aging, 8: 1089-1095.

40. Wang JQ, Yin J, Song YF, Zhang L, Ren YX, Wang DG, Gao LP and Jing YH (2014): Brain aging and AD-like pathology in streptozotocin-induced diabetic rats. J Diabetes Res, 2014: 796840-796851.

41. Nazem A, Sankowski R, Bacher M and Al-Abed Y (2015): Rodent models of neuroinflammation for Alzheimer's disease. J Neuroinflammation, 12: 74-88.

42. Castellani RJ and Perry G (2014): The complexities of the pathology–pathogenesis relationship in Alzheimer disease. Biochem Pharmacol, 88(4): 671-676.

43. Wang D and Mitchell ES (2016) : Cognition and Synaptic-Plasticity Related Changes in Aged Rats Supplemented with 8- and 10-Carbon Medium Chain Triglycerides. PLoS One, 11:e0160159-0160174.

44. Wang XP, Ye P, Lv J, Zhou L, Qian ZY, Huang YJ, Mu ZH, Wang X, Liu XJ, Wan Q, Yang ZH, Wang F and Zou YY (2019): Expression Changes of NMDA and AMPA Receptor Subunits in the Hippocampus in rats with Diabetes Induced by Streptozotocin Coupled with Memory Impairment. Neurochem Res, 44(4): 978-993.

45. Rachmany L, Tweedie D, Rubovitch V, Li Y, Holloway HW, Kim DS, Ratliff DA, Saykally JN, Citron BA, Hoffer BJ, Greig NH and Pick CG (2017): Exendin-4 attenuates blast traumatic brain injury induced cognitive impairments, losses of synaptophysin and in *vitro* TBI-induced hippocampal cellular degeneration. Sci Rep, 7(1): 3735-3765.

46. Ma S, Xie N, Li W, Yuan B, Shi Y and Wang Y (2014): Immunobiology of mesenchymal stem cells. Cell Death Differ, 21: 216-225.

47. Vono R, Fuoco C, Testa S, Pirrò S, Maselli D, Ferland McCollough D, Sangalli E, Pintus G, Giordo R, Finzi G, Sessa F, Cardani R, Gotti A, Losa S, Cesareni G, Rizzi R, Bearzi C, Cannata S, Spinetti G, Gargioli C and Madeddu P (2016): Activation of the Pro-Oxidant PKCβII-p66Shc Signaling Pathway Contributes to Pericyte Dysfunction in Skeletal Muscles of Patients With Diabetes With Critical Limb Ischemia. Diabetes, 65(12):3691-3704.

48. Gerace D, Martiniello-Wilks R, Nassif NT, Lal S, Steptoe R and Simpson AM (2017): CRISPR-targeted genome editing of mesenchymal stem cell-derived therapies for type 1 diabetes: a path to clinical success? Stem Cell Res Ther, 8(1):62-71.

49. Lin W, Xu L, Zwingenberger S, Gibon E, Goodman SB and Li G (2017): Mesenchymal stem cells homing to improve bone healing. Journal of Orthopaedic Translation, 9: 19-27.

50. Ding SLS, Kumar S and Mok PL (2017): Cellular Reparative Mechanisms of Mesenchymal Stem Cells for Retinal Diseases. Int J Mol Sci, 18(8): 1406-1424.

51. Moretti M, Fraga DB and Rodrigues ALS (2017): Preventive and therapeutic potential of ascorbic acid in neurodegenerative disease. CNS Neurosci Ther, 23(12): 921-929.

52. Sil S, Ghosh T, Gupta P, Ghosh R, Kabir SN and Roy A (2016): Dual role of vitamin C on the neuroinflammation mediated neurodegeneration and memory impairments in Colchicine induced rat model of Alzheimer Disease. J Mol Neurosci, 60: 421-435.

53. Oyarce K, Silva-Alvarez C, Ferrada L, Martínez F, Salazar K and Nualart F (2017): SVCT2 Is Expressed by Cerebellar Precursor Cells, Which Differentiate into Neurons in Response to Ascorbic Acid. Mol Neurobiol, 55(2): 1136-1149.

54. Luo Y, Cheng YW, Yu CY, Liu RM, Zhao YJ, Chen DX, Zhong JJ, and Xiao JH (2019): Effects of hyaluronic acid on differentiation of human amniotic epithelial cells and cell-replacement therapy in type 1 diabetic mice. Exp Cell Res, 384(2): 111642.

55. Mahmoud EE, Adachi N, Mawas AS, Deie M and Ochi M (2019): Multiple intra-articular injections of allogeneic bone marrow-derived stem cells potentially improve knee lesions resulting from surgically induced osteoarthritis: an animal study. Bone Joint J, 101-B(7):824-831.

56. Fan X, Sun D, Tang X, Cai Y, Yin ZQ and Xu H (2014): Stem-cell challenges in the treatment of Alzheimer's disease: a long way from bench to bedside. Med Res Rev, 34(5): 957-978.

57. Kim S, Chang K, Kim J, Park H, Ra J, Kim H and Suh Y (2012): The Preventive and Therapeutic Effects of Intravenous Human Adipose-Derived Stem Cells in Alzheimer's disease Mice. PLoS One, 7(9): 45757- 45773.

58. Devitt SM, Carter CM, Dierov R, Weiss S, Gersch RP and Percec I (2015): Successful Isolation of Viable Adipose-Derived Stem Cells from Human Adipose Tissue Subject to Long-Term Cryopreservation: Positive Implications for Adult Stem Cell-Based Therapeutics in Patients of Advanced Age. Stem Cells Int, 2015: 146421-146431.

59. Mizuno H, Tobita M and Uysal AC (2012): Concise review: Adipose-derived stem cells as a novel tool for future regenerative medicine. Stem Cells, 30(5): 804-810.

60. Liu L, Eckert MA, Riazifar H, Kang DK, Agalliu D and Zhao W (2013): From blood to the brain: can systemically transplanted mesenchymal stem cells cross the blood-brain barrier? Stem Cells Int, 2013: 435093-435099.

61. Lykhmus O, Koval L, Voytenko L, Uspenska K, Komisarenko S, Deryabina O, Shuvalova N, Kordium V, Ustymenko A, Kyryk V, Skok M (2019): Intravenously Injected Mesenchymal Stem Cells Penetrate the Brain and Treat Inflammation-Induced Brain Damage and Memory Impairment in Mice. Front Pharmacol, 10: 355.

<div dir="rtl">

الملخص العربى

تأثير الحقن المفرد والمتعدد للخلايا الجذعية الدهنية وحمض الأسكوربيك على القشرة المخية: دراسة نسيجية في داء السكري من النوع الأول المستحث تجريبياً

مها بليغ زكرى¹، داليا حسين عبد العزيز²، أسماء محمود مصطفى²، عزه صالح امبابي²

قسم الهستولوجيا الطبيه وبيولوجيا الخليه، كلية الطب، ¹جامعة القاهره و²جامعة بني سويف، مصر

الخلفية والأهداف: مرض الزهايمر هو سبب شائع للخرف في العالم. الارتباط بين مرض السكري ومرض الزهايمر قوي جدًا لدرجة أن مرض الزهايمر يُشار إليه بمرض السكري في الدماغ وقد لعبت الخلايا الجذعية الدهنية دورًا أساسي في زرع الخلايا الجذعية في النماذج الحيوانية. هدفت الدراسة الحالية الى تقيم ومقارنة الأثر المحتمل لكلا من الحقن المفرد والمتعدد للخلايا الجذعية الدهنية والدور المحتمل لحمض الأسكوربيك على القشرة الدماغية في ذكر الجرذ الأبيض البالغ المصاب بداء السكري.

الادوات و الطرق: وقد شملت هذه الدراسه إستخدام أربعة وأربعون جرذا بالغا ذكرا تم تقسيمهم الى: المجموعة الأولى (المجموعة الضابطة): خمسة جرذان, المجموعة الثانية (المجموعة المصابة بالسكري)، المجموعة الثالثة (المجموعة المصابة بالسكري ومعالجة بالحقن المفرد للخلايا الجذعية الدهنية)، المجموعة الرابعة (المجموعة المصابة بالسكري ومعالجة بالحقن المفرد للخلايا الجذعية الدهنية مع حمض الأسكوربيك): كل مجموعة تشمل ٧ جرذان، تم حقن كل منها بالستربتوزتوسين مرة واحدة في الغشاء البريتوني بجرعة ٥٠ مجم/ كجم. في المجموعة الثالثة والرابعة تم حقن ١٠٦×١ خلايا جذعية دهنية في الوريد الذيلي للجرذان. في المجموعة الرابعة تم اضافة ٥٠٠ ميللي جرام/كيلوجرام حمض الأسكوربيك عن طريق الفم. المجموعة الخامسة (المجموعة المصابة بالسكري ومعالجة بالحقن المتعدد للخلايا الجذعية الدهنية)، المجموعة السادسة (المجموعة المصابة بالسكري ومعالجة بالحقن المتعدد للخلايا الجذعية الدهنية مع حمض الأسكوربيك): كل مجموعة تشمل ٧ جرذان. تم حقن كل منها ١ميللي من الخلايا الجذعية الدهنية أربع مرات عن طريق الوريد. في المجموعة السادسة مصاحب يوميا بجرعة حمض الأسكوربك عن طريق الفم.

شملت هذه الدراسات: دراسة هستولوجية، هستوكيميائية، هستوكيميائية مناعية، كمية قياسية وتحليل احصائي.

ومن نتائج هذه الدراسة تبين ما يلي: أظهرت المجموعة الثانية كتلًا كبيرة متعددة تظهر انويه مظلمة في الطبقة الهرمية الخارجية (EP)، والخلايا العصبية المشوهة، مع وجود خلخله عصبيه.

المجموعة الثالثة أظهرت تحسن طفيف فى التغيرات السابقة. المجموعة الرابعة أوضحت تغيرات افضل. المجموعة الخامسة أظهرت تحسن ملحوظ بينما المجموعة السادسة أوضحت تغيرات قليلة.

الخلاصه: مرض السكري النوع الأول يستحث تغيرات تنكسية والتهابية في القشرة الخارجية للمخ. وقد أثبتت الخلايا الجذعية الدهنية تأثيرا علاجيا ملحوظا أكثر في الحقن المتعدد.

العلاج المشترك بين الخلايا الجذعية وحمض الاسكوربيك يضمن التأثير الأكثر فاعليه وقد يعود السبب لتنشيط هجرة وتمايز الخلايا.

</div>